

Research Article

Structural and Thermal Stability of Sol-Gel Prepared $\text{MgHf}_4\text{P}_6\text{O}_{24}$ Solid Electrolyte in Molten Pure Aluminium

^{a,b,c,*}**Mohammed Alhaji Adamu and ^cGirish M Kale**

^aDepartment of Metallurgical and Materials Engineering Technology, Kogi State Polytechnic, Lokoja, Nigeria

^bEngineering Materials Research Group, Kogi State Polytechnic, Lokoja, Nigeria

^cSchool of Chemical and Process Engineering, University of Leeds, Leeds LS2 9JT, United Kingdom

*Corresponding Author Email: drmadamu@yahoo.com

Received: August 17, 2025

Accepted: September 06, 2025

Published: September 12, 2025

Abstract

The potential solid electrolyte, $\text{MgHf}_4\text{P}_6\text{O}_{24}$ was prepared using modified novel sol-gel process. Structural and thermal stability properties of the solid electrolyte were determined. TGA-DSC and HT-XRD analyses indicated that the pure dried xerogel powder, when calcined at 900 °C converts to pure homogeneous single phase $\text{MgHf}_4\text{P}_6\text{O}_{24}$ nanopowders with good crystallinity. Pellets of 13 mm diameter and 3.8 mm thickness made by uniaxial compression were sintered at 1300 °C. XRD analysis indicated that the crystalline phase is monoclinic, with a crystallite size of approximately 42 nm. The sintered pellets were stable in the temperature range from 1000 °C to 1300 °C, with no trace of coexistent second phase peaks at higher temperatures. Relative density analysis of $\text{MgHf}_4\text{P}_6\text{O}_{24}$ pellets yielded an optimum density and porosity of about 98% and 2%, respectively at 1300 °C. The dense pellet, dipped into pure molten Al at 700 ± 5 °C for 8 h, exhibits impressive structural and thermal stability, showing no single trace of extraneous phase formation. This portrays $\text{MgHf}_4\text{P}_6\text{O}_{24}$ as a solid electrolyte with suitable application in high-temperature electrochemical devices.

Keywords: Sol-Gel Process, Solid Electrolyte, X-Ray Diffraction, Relative Density, Molten Al.

1. Introduction

Phosphate based solid electrolytes have been widely studied due to their suitability as solid electrolyte in electrochemical devices and thermodynamic measurements (Adamu and Kale, 2016), and it has become a focus of attention for its high ionic conductivity which is appropriate for designing high-temperature electrochemical Mg-sensors (Adamu *et al.*, 2020), solid-state Mg-based batteries (Pang *et al.*, 2023), fundamental thermodynamic investigations at elevated temperatures in aggressive environment (Pet'kov *et al.*, 2014; Mudenda and Kale, 2017; Sivasankaran and Kumar, 2019), microwave dielectric materials (Li *et al.*, 2020). Different methods have been used in producing phosphate-based solid electrolytes; solid-state method (Tamura *et al.*, 2016) and sol-gel method (Mustaffa and Mohamed, 2016; Shetti *et al.*, 2017) have yielded solid electrolytes in which the electric current is predominantly by ions (Ipser *et al.*, 2010). Magnesium phosphate solid electrolytes like other nanoceramic materials possess high density and thermal stability, able to be produced into variety of sizes and shapes having an ordered structure compared to liquid electrolytes (Sardar *et al.*, 2020).

The sol-gel method is believed to be an excellent method for producing pure $\text{MgHf}_4\text{P}_6\text{O}_{24}$ xerogel powders from precursor oxides of high purity and uniform composition. In an earlier study, the potential advantages of sol-gel synthesis over conventional solid-state reaction was identified to include improved homogeneity, better compositional control and lower processing temperatures (Kakihana, 1996; Brinker and Scherer, 2013). Sol-gel method has also produced homogeneous dense ceramic materials at low ambient temperatures (Joost and Krajewski, 2017; Judez *et al.*, 2018) compared to the conventional solid-state reaction (Tamura *et al.*, 2016) which is achieved at high temperatures, thereby reducing carbon footprints.

In a previous study, phosphate-based solid electrolytes have found suitable applications in Mg-sensors and other electrochemical devices which have been extensively discussed (Pratt, 1990; Ferloni and Magistris, 1994; Chang and Sommer, 1997; Kale *et al.*, 2004; Fergus, 2009). Potential application of solid electrolytes in

electrochemical Mg-sensors, rechargeable energy sources, and storage systems such as solid-state batteries for electrical vehicles is the signature need for increasing future demands for phosphate-based $\text{MgHf}_4\text{P}_6\text{O}_{24}$ solid electrolytes. In this study, a series of structural and thermal characterisation techniques were used to analyse the structural stability of $\text{MgHf}_4\text{P}_6\text{O}_{24}$ solid electrolyte from room temperature up to 1500 °C, and thermal behaviour of the solid electrolyte in molten pure aluminium at 700 ± 5 °C for 8 h.

2. Materials and Methods

2.1. Materials Synthesis

Figure 1 shows the preparation route of $\text{MgHf}_4\text{P}_6\text{O}_{24}$ solid electrolyte using sol-gel method. This method produced a pure, fine nanopowders; achieved through mixing on atomic scale by combining aqueous solutions of soluble salts of magnesium, hafnium and phosphorous in an elemental ratio of 1:4:6 at 50 °C on a hot plate with installed magnetic stirring while NH_4OH was added dropwise to the homogeneous gel to neutralise its pH from 0.2 acidic to 8.9 alkali at a relatively low crystallisation temperature and it produced compositions not always possible by the solid-state fusion method. The starting reagents in this study; $\text{Mg}(\text{NO}_3)_2$ dried powder (Sigma-Aldrich Chemical Co Ltd; Gillingham, Dorset, UK), HfCl_4 and $\text{NH}_4\text{H}_2\text{PO}_4$ (Alfa Aesar Fine Chemicals and Metals; Heysham, Lancashire, UK) were weighed in stoichiometric proportions and dissolved in deionised H_2O . The final solution was stirred for 1 h and dried on a hot plate at 100 °C. After drying, the resultant xerogel powder was mechanically ground into homogeneous xerogel powder with fine particle size using agate mortar and pestle. The stoichiometric reaction and flowchart showing sol-gel synthesis of prepared $\text{MgHf}_4\text{P}_6\text{O}_{24}$ solid electrolyte are presented in Equation 1 and Figure 1, respectively.

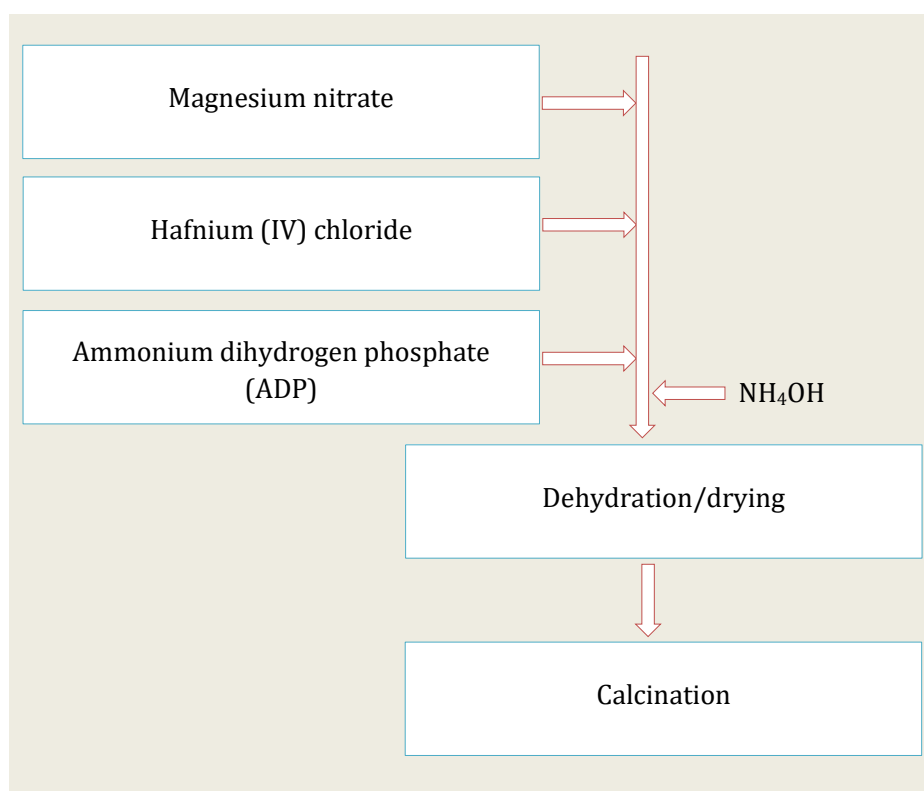
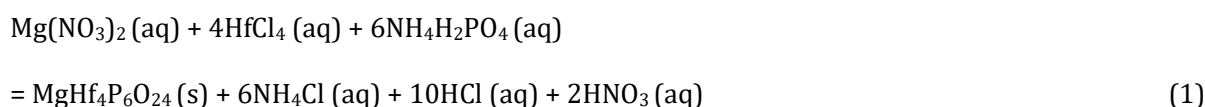


Figure 1. Flowchart showing the sol-gel synthesis procedures of prepared $\text{MgHf}_4\text{P}_6\text{O}_{24}$ solid electrolyte.

2.2. Materials Characterisation

Homogeneous xerogel powders were subjected to thermal analysis; thermogravimetric analysis and differential scanning calorimetry (TGA-DSC) using STA 8000 (PerkinElmer, Seer Green, UK) for the purpose of measuring thermal oxidation behaviour and weight loss of the pure dried xerogel powders. The analysis ensured effective optimisation of calcination conditions of the xerogel powder in a controlled atmosphere at a flow rate of 50 mL min^{-1} using a constant heating-cooling rate at 10 °C min^{-1} from 30 °C to 1000 °C, akin to those described in previous studies (Adamu and Kale, 2016; Adamu *et al.*, 2020). The resultant dried xerogel powders were calcined at 900 °C, and then pressed into pellets of 13 mm diameter and 3.8 mm thickness

with a uniaxial compression. The resultant pellets were then sintered at 1300 °C in a closed alumina crucible immersed in powders of the calcined sample composition.

The structural characterisation, phase identification and average crystallite size (D) of the solid electrolyte was analysed by XRD. The calcined $\text{MgHf}_4\text{P}_6\text{O}_{24}$ nanopowders and sintered pellets were analysed using x-ray powder diffraction (Bruker D8 diffractometer, with $\text{Cu-K}\alpha$ X-rays). High-temperature x-ray diffraction, HT-XRD (PANalytical X'pert diffractometer) was used to analyse the phase and structural behaviour of the prepared xerogel powders at temperatures ranging from 25 °C to 900 °C.

Alumina tubes of 125 mm long were used to prepare the $\text{MgHf}_4\text{P}_6\text{O}_{24}$ solid electrolyte probes for thermal stability testing in pure molten Al at 700 ± 5 °C for 8 h. Dense pellet of $\text{MgHf}_4\text{P}_6\text{O}_{24}$ solid electrolyte was held firmly onto one opened end alumina tubes with pure alumina refractory cement (Parkinson-Spencer Refractories Ltd., Halifax, UK) to prepare the probe for stability testing.

3. Results and Discussion

3.1. Thermal Analysis (TGA-DSC)

Thermal stability of the $\text{MgHf}_4\text{P}_6\text{O}_{24}$ precursor xerogel powder was analysed using TGA-DSC. The main decomposition changes on the TGA profiles in Figure 2 is presented in three regions: the first region ranging from 30 °C to 100 °C corresponds to the dehydration of lattice H_2O . The weight loss in a temperature region from 150 °C to 500 °C is due to the decomposition or oxidation of the gelled inorganic precursors; $\text{Mg}(\text{NO}_3)_2$, HfCl_4 and $\text{NH}_4\text{H}_2\text{PO}_4$. There was no further reduction in weight above 500 ± 25 °C for $\text{MgHf}_4\text{P}_6\text{O}_{24}$ xerogel powders. Similarly, the DSC profiles of $\text{MgHf}_4\text{P}_6\text{O}_{24}$ xerogel powders in Figure 2 clearly identifies two endothermic decomposition peaks at 150 °C and 350 °C, and an exothermic peak at 900 °C.

The phosphate precursor, $\text{NH}_4\text{H}_2\text{PO}_4$ decomposes into $(\text{NH}_4)_3\text{H}_2\text{P}_3\text{O}_{10}$ and H_2O molecules at temperatures ranging from 140 °C to 170 °C which could be responsible for the endothermic peak seen at 150 °C. The inorganic precursor, $\text{Mg}(\text{NO}_3)_2$ also decomposes into MgO , NO_2 and O_2 at a temperature above 300 °C, which could be responsible for the endothermic peak at 350 °C. The reactive oxide HfO_2 formed by the oxidation of HfCl_4 at 432 °C results in the formation of $\text{MgHf}_4\text{P}_6\text{O}_{24}$ solid electrolyte after stoichiometric reaction with MgO and P_2O_5 reactive oxides at 900 °C. Therefore, the exothermic peak observed at 900 °C shows the formation of a single phase $\text{MgHf}_4\text{P}_6\text{O}_{24}$ solid electrolyte with excellent crystallinity. The formation of a single phase $\text{MgHf}_4\text{P}_6\text{O}_{24}$ solid electrolyte started at 780 °C as indicated on the TGA profile.

The TGA-DSC analysis in this study could not exceed 1000 °C because of the temperature limitation of the STA 8000 equipment used. However, it was observed that no extraneous peak manifests on the DSC profile at higher temperatures.

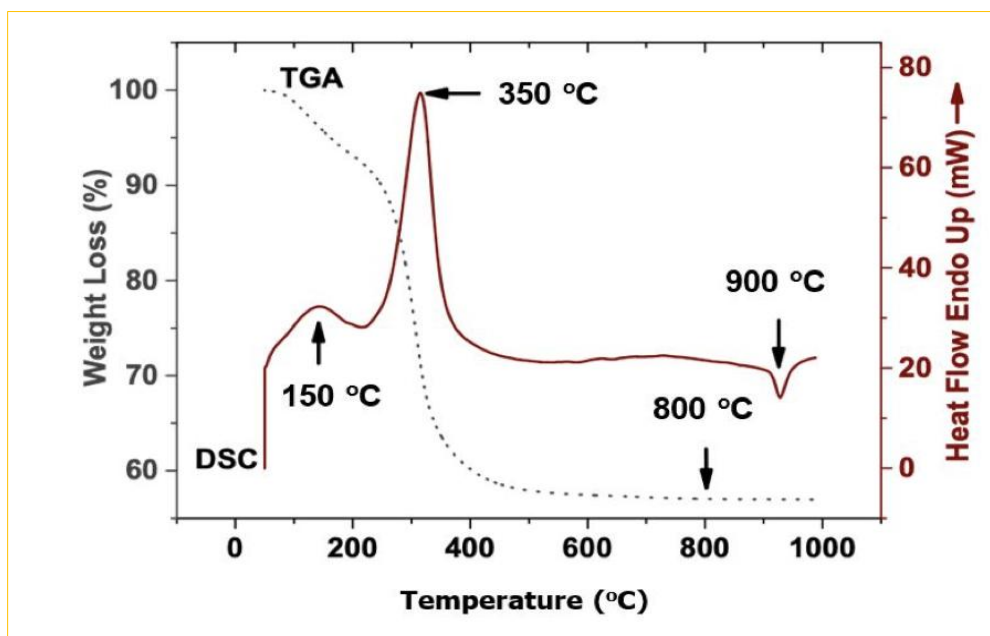


Figure 2. TGA-DSC profiles of $\text{MgHf}_4\text{P}_6\text{O}_{24}$ dried xerogel powders at a uniform scan rate of $10\text{ }^{\circ}\text{C min}^{-1}$ in the air.

3.2. High-Temperature X-Ray Diffraction (HT-XRD)

Figure 3 shows HT-XRD analysis of $\text{MgHf}_4\text{P}_6\text{O}_{24}$ xerogel powders at different crystallisation temperatures. The HT-XRD patterns predicted the formation of $\text{MgHf}_4\text{P}_6\text{O}_{24}$ solid electrolyte at 900 °C, with all of the peaks matched and properly indexed.

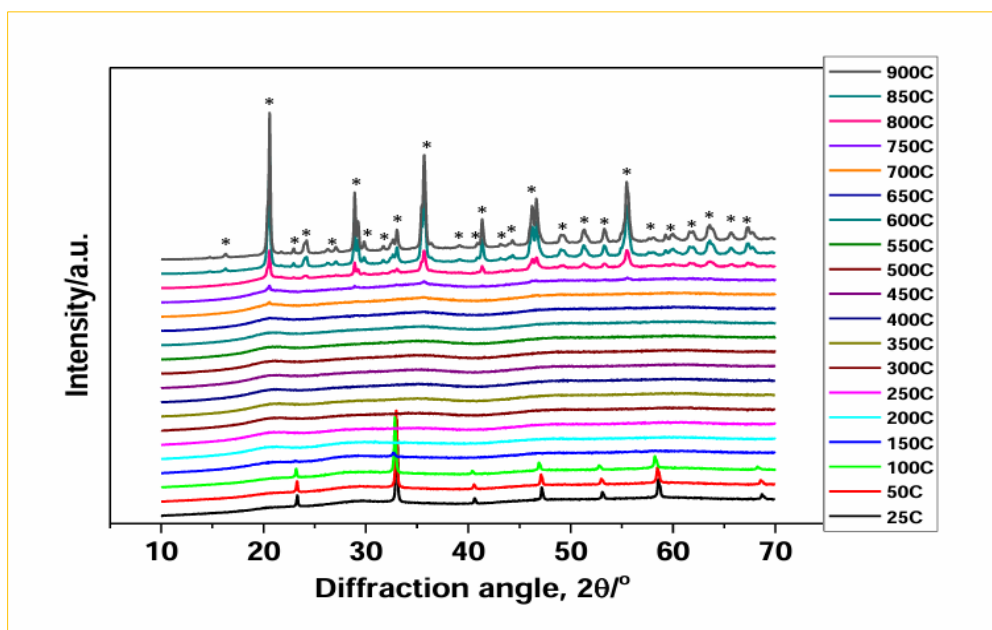


Figure 3. High-temperature XRD profiles for $\text{MgHf}_4\text{P}_6\text{O}_{24}$ xerogel powders (*crystalline peak profiles of $\text{MgHf}_4\text{P}_6\text{O}_{24}$ solid electrolytes).

3.3. Powder X-Ray Diffraction (XRD)

Based on the thermal analysis (TGA-DSC) reported for $\text{MgHf}_4\text{P}_6\text{O}_{24}$ dried xerogel powders in Figure 2, single phase $\text{MgHf}_4\text{P}_6\text{O}_{24}$ solid electrolyte was formed by calcining the dried xerogel powders at 900 °C. Powder x-ray diffraction (XRD) analysis was used as an alternative tool for measuring thermal stability of $\text{MgHf}_4\text{P}_6\text{O}_{24}$ dried xerogel powders akin to the thermal analysis in an earlier study (Adamu and Kale, 2016; Adamu *et al.*, 2020). In addition, 1300 °C was considered the sintering temperature of $\text{MgHf}_4\text{P}_6\text{O}_{24}$ solid electrolyte because dense and stable pellets were achieved at that temperature. Figure 4 shows the pure single phase nanopowders calcined at 900 °C and pellets sintered at 1300 °C, and their peaks were properly indexed.

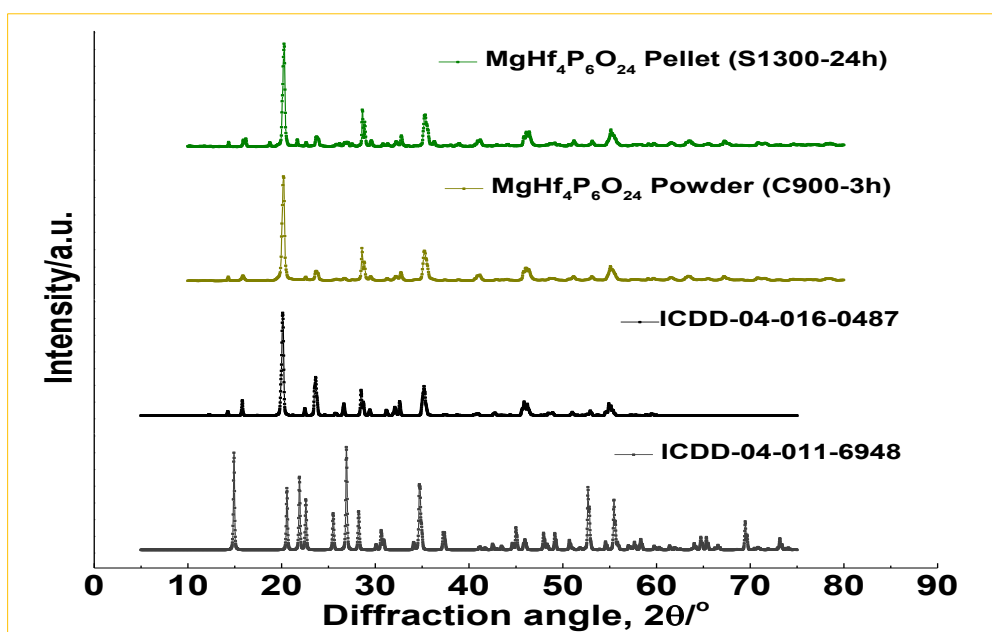


Figure 4. X-ray diffraction peaks of $\text{MgHf}_4\text{P}_6\text{O}_{24}$ nanopowders calcined at 900 °C and pellets sintered at 1300 °C. All peaks were indexed to $\text{Mg}_{0.5}\text{Zr}_2(\text{PO}_4)_3$ [ICDD-04-016-0487] and $\text{Zr}_2(\text{PO}_4)_2\text{O}$ [ICDD-04-011-6948].

3.4. Relative Density and Porosity

The relative density of solid electrolytes is proportional to sintering temperature at a constant annealing time. In Figure 5, the $\text{MgHf}_4\text{P}_6\text{O}_{24}$ solid electrolyte shows about 95% relative density at temperature higher than 1100 °C and an optimum relative density of about 98% at 1300 °C. The optimum relative density of approximately 98% achieved for $\text{MgHf}_4\text{P}_6\text{O}_{24}$ solid electrolyte agrees with the assertion that acceptable relative density of solid electrolytes should be higher than 94% (Mori *et al.*, 2006). The increment in density from 1300 °C to 1500 °C is about 1%, signifying that a saturation point has been reached for the densification. The porosity of about 2% was also achieved at 1300 °C as observed in Figure 5, which is perfect for solid electrolytes in electrochemical applications.

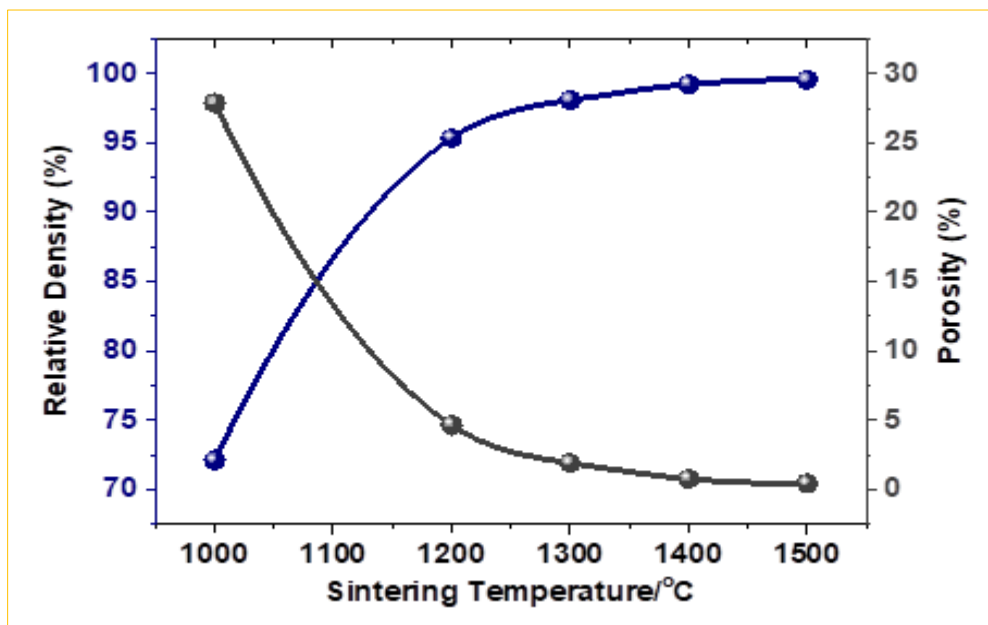


Figure 5. Dependence of relative density and porosity of $\text{MgHf}_4\text{P}_6\text{O}_{24}$ solid electrolyte on sintering temperature.

3.5. Thermal Stability Testing

Testing for stability is meant to investigate the stability of $\text{MgHf}_4\text{P}_6\text{O}_{24}$ solid electrolytes in molten Al. Stability testing of the solid electrolytes in pure molten Al was done at 700 ± 5 °C for 8 h, in a pure alumina crucible using top-loading Lenton LTF1600 muffle furnace (Lenton Thermal Designs Ltd., Market Harborough, UK) shown in Figure 6. The prepared probes were dipped into pure molten Al at 700 ± 5 °C for 8 h, inside the top-loading Lenton LTF1600 muffle furnace described in Figure 6. The molten Al is covered by a thin layer of eutectic NaCl-KCl salts that prevents oxidation of the molten Al at high-temperatures. The molten Al at 700 ± 5 °C is sufficient for melting the eutectic NaCl-KCl salts with a minimum melting temperature of 657 °C. Figure 7 shows the XRD profiles of $\text{MgHf}_4\text{P}_6\text{O}_{24}$ solid electrolyte immersed in molten Al at 700 ± 5 °C for 8 h. This profiles compare well with the peaks indexed in Figure 4 which implies that the solid electrolyte possesses impressive structural and thermal stability in molten Al at 700 ± 5 °C for 8 h.

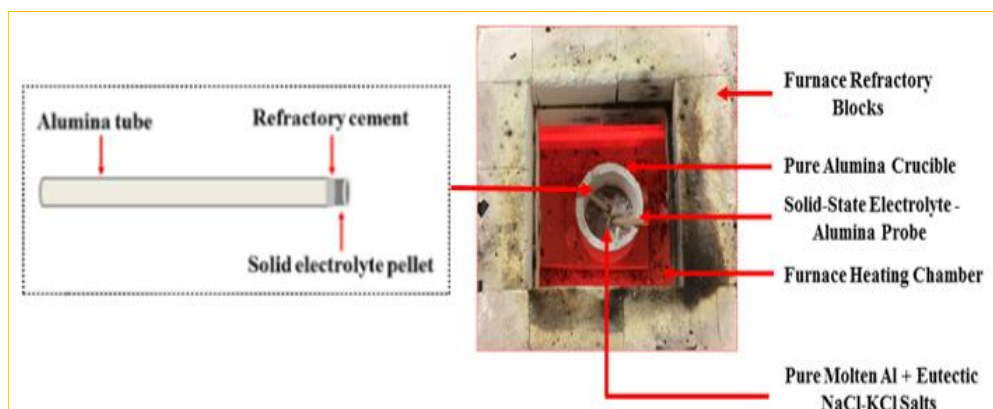


Figure 6. Stability testing of $\text{MgHf}_4\text{P}_6\text{O}_{24}$ solid electrolyte pellets in molten Al at 700 ± 5 °C for 8 h using top-loading Lenton LTF 1600 muffle furnace.

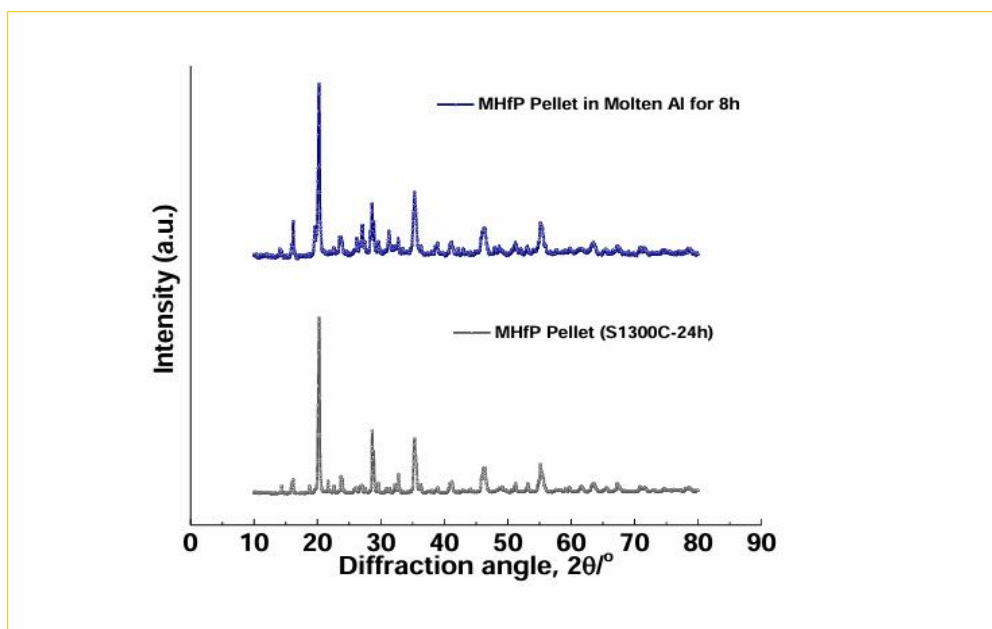


Figure 7. Stability testing of the $\text{MgHf}_4\text{P}_6\text{O}_{24}$ solid electrolyte in molten pure Al for 8 h.

4. Conclusion

Based on the TGA-DSC and HT-XRD analyses, the dried pure xerogel powders were calcined at 900 °C to produce a single phase $\text{MgHf}_4\text{P}_6\text{O}_{24}$ solid electrolyte of definite crystallinity. High-temperature x-ray diffraction further validated the formation of a single phase at 900 °C and 1300 °C which affirms that $\text{MgHf}_4\text{P}_6\text{O}_{24}$ solid electrolyte remains stable at high temperatures. In addition, the structural and thermal stability of $\text{MgHf}_4\text{P}_6\text{O}_{24}$ solid electrolyte at high temperatures make it suitable for application in high-temperature electrochemical devices.

Declarations

Acknowledgments: The authors would like to acknowledge the School of Chemical and Process Engineering, University of Leeds, United Kingdom for the world class facilities provided for this study. Profound appreciation also goes to the Tertiary Education Trust Fund (TETFund) and Kogi State Polytechnic, Lokoja, Nigeria for funding this novel research interest.

Author Contributions: MAA: Study conception and design, data collection, analysis and interpretation of results, manuscript preparation and submission of article; GMK: Manuscript revision and editing.

Conflict of Interest: The authors declare no conflict of interest.

Consent to Publish: The authors agree to publish the paper in International Journal of Recent Innovations in Academic Research.

Data Availability Statement: All relevant data are included in the manuscript.

Funding: This research was funded by the Tertiary Education Trust Fund (TETFund) and Kogi State Polytechnic, Lokoja, Nigeria in the form of Academic Staff Training and Development (PhD Student Grant 2013-2016).

Institutional Review Board Statement: Not applicable.

Informed Consent Statement: Not applicable.

Research Content: The research content of the manuscript is original and has not been published elsewhere.

References

1. Adamu, M. and Kale, G.M. 2016. Novel sol-gel synthesis of $\text{MgZr}_4\text{P}_6\text{O}_{24}$ composite solid electrolyte and newer insight into the Mg^{2+} -ion conducting properties using impedance spectroscopy. *Journal of Physical Chemistry C*, 120(32): 17909-17915.
2. Adamu, M., Jacob, K.T. and Kale, G.M. 2020. Assessment of $\text{MgZr}_4\text{P}_6\text{O}_{24}$ as a solid electrolyte for sensing Mg in molten non-ferrous alloys. *Journal of the Electrochemical Society*, 167(2): 027532.
3. Brinker, C.J. and Scherer, G.W. 2013. *Sol-gel science: The physics and chemistry of sol-gel processing*. Academic Press, New York, 912p.
4. Chang, Y.A. and Sommer, F. 1997. Thermodynamics of alloy formation. In: TMS 1997. Warrendale, 77p.

5. Fergus, J.W. 2009. Electrochemical sensors: Fundamentals, key materials and applications. (Eds.), Kharton, V.V., Solid state electrochemistry I: Fundamentals, materials and their applications, 427-491pp.
6. Ferloni, P. and Magistris, A. 1994. New materials for solid state electrochemistry. Journal de Physique IV France, 4(C1): C1-3 -C1-15.
7. Ipser, H., Mikula, A. and Katayama, I. 2010. Overview: The emf method as a source of experimental thermodynamic data. Calphad, 34(3): 271-278.
8. Joost, W.J. and Krajewski, P.E. 2017. Towards magnesium alloys for high-volume automotive applications. Scripta Materialia, 128: 107-112.
9. Judez, X., Zhang, H., Li, C., Eshetu, G.G., Gonzalez-Marcos, J.A., Armand, M. and Rodriguez-Martinez, L.M. 2018. Solid electrolytes for safe and high energy density lithium-sulfur batteries: Promises and challenges. Journal of the Electrochemical Society, 165(1): A6008-A6016.
10. Kakihana, M. 1996. Invited review "sol-gel" preparation of high temperature superconducting oxides. Journal of Sol-Gel Science and Technology, 6(1): 7-55.
11. Kale, G.M., Wang, L. and Hong, Y. 2004. High-temperature sensor for in-line monitoring of Mg and Li in molten Al employing ion-conducting ceramic electrolytes. International Journal of Applied Ceramic Technology, 1(2): 180-187.
12. Li, M., Li, X., Gong, W., Chen, P. and Zhu, B. 2020. Tunability study on microstructure and electromagnetic properties of Ce-doped $\text{MgZr}_4\text{P}_6\text{O}_{24}$. Journal of Alloys and Compounds, 820: 153097.
13. Mori, M., Suda, E., Pacaud, B., Murai, K. and Moriga, T. 2006. Effect of components in electrodes on sintering characteristics of $\text{Ce}_{0.9}\text{Gd}_{0.1}\text{O}_{1.95}$ electrolyte in intermediate-temperature solid oxide fuel cells during fabrication. Journal of Power Sources, 157(2): 688-694.
14. Mudenda, S. and Kale, G.M. 2017. Electrochemical determination of activity of Na_2O in $\text{Na}_2\text{Ti}_6\text{O}_{13}$ - TiO_2 two phase system between 803-1000 K. Electrochimica Acta, 258: 1059-1063.
15. Mustaffa, N.A. and Mohamed, N.S. 2016. Zirconium-substituted $\text{LiSn}_2\text{P}_3\text{O}_{12}$ solid electrolyte prepared via sol-gel method. Journal of Sol-Gel Science and Technology, 77(3): 585-593.
16. Pang, Y., Zhu, Y., Fang, F., Sun, D. and Zheng, S. 2023. Advances in solid Mg-ion electrolytes for solid-state Mg batteries. Journal of Materials Science and Technology, 161: 136-149.
17. Pet'kov, V.I., Shipilov, A.S., Markin, A.V. and Smirnova, N.N. 2014. Thermodynamic properties of crystalline magnesium zirconium phosphate. Journal of Thermal Analysis and Calorimetry, 115(2): 1453-1463.
18. Pratt, J.N. 1990. Applications of solid electrolytes in thermodynamic studies of materials: A review. Metallurgical and Materials Transactions A, 21: 1223-1250.
19. Sardar, S., Kale, G.M. and Ghadiri, M. 2020. Influence of processing conditions on the ionic conductivity of holmium zirconate ($\text{Ho}_2\text{Zr}_2\text{O}_7$). Ceramics International, 46(8 Part B): 11508-11514.
20. Shetti, N.P., Nayak, D.S., Malode, S.J. and Kulkarni, R.M. 2017. Electrochemical sensor based upon ruthenium doped TiO_2 nanoparticles for the determination of flufenamic acid. Journal of the Electrochemical Society, 164(5): B3036-B3042.
21. Sivasankaran, U. and Kumar, K.G. 2019. Electrochemical sensing of synthetic antioxidant propyl gallate: A cost-effective strategy using nanoparticles. Journal of the Electrochemical Society, 166(2): B92.
22. Tamura, S., Yamane, M., Hoshino, Y. and Imanaka, N. 2016. Highly conducting divalent Mg^{2+} cation solid electrolyte with well-ordered three-dimensional network structure. Journal of Solid State Chemistry, 235: 7-11.

Citation: Mohammed Alhaji Adamu and Girish M Kale. 2025. Structural and Thermal Stability of Sol-Gel Prepared $\text{MgHf}_4\text{P}_6\text{O}_{24}$ Solid Electrolyte in Molten Pure Aluminium. International Journal of Recent Innovations in Academic Research, 9(3): 294-300.

Copyright: ©2025 Mohammed Alhaji Adamu and Girish M Kale. This is an open-access article distributed under the terms of the Creative Commons Attribution License (<https://creativecommons.org/licenses/by/4.0/>), which permits unrestricted use, distribution, and reproduction in any medium, provided the original author and source are credited.